IEEE Access
Multidisciplinary | Rapid Review | Open Access Journal

Received March 5, 2020, accepted March 28, 2020, date of publication April 3, 2020, date of current version April 20, 2020.

Digital Object Identifier 10.1109/ACCESS.2020.2985384

MINLOC:Magnetic Field Patterns-Based Indoor Localization Using Convolutional Neural Networks

IMRAN ASHRAF, MINGYU KANG, SOOJUNG HUR, AND YONGWAN PARK
Department of Information and Communication Engineering, Yeungnam University, Gyeongsan 38544, South Korea

Corresponding author: Yongwan Park (ywpark@yu.ac.kr)

This work was supported in part by the Ministry of Science (MSIT) and ICT, South Korea, through the Information Technology Research Center (ITRC) supervised by the Institute for Information and Communications Technology Promotion (IITP) under Grant IITP-2019-2016-0-00313, and in part by the 2019 Yeungnam University Research Grant.

ABSTRACT Conventional geomagnetic field-based indoor positioning and localization techniques determine the user's position by comparing the database with the geomagnetic field strength collected by the user. However, the magnetic field strength collected from various devices varies significantly. So, the greater the difference between the geomagnetic field strength stored in the database and user collected geomagnetic field strength is, the lower the degree of location accuracy will be. The diversity of smartphone makes it impossible to develop a single database which can work with all the smartphones in the same fashion. Intending to solve these problems, this paper proposes the use of geomagnetic field patterns called MP (Magnetic Pattern) with CNN (Convolutional Neural Networks) to perform indoor localization. The database is constructed using the MP that occurs at the points of measurement while the location is calculated using CNN which matches the user collected MP with the database. A voting mechanism is contrived to combine the predictions from several CNNs and the user's position is finally estimated. To evaluate the performance of the proposed technique, Samsung Galaxy S8 and LG G6 are used in two buildings with different experimental environments and path geometry. The proposed approach is tested by two male and two female users for analyzing the impact of user heights. Experiment results show promising results; furthermore, the comparison analysis with other magnetic indoor localization approaches demonstrate that the proposed approach outperforms them.

INDEX TERMS Indoor localization, convolutional neural networks, magnetic field data, pedestrian dead reckoning, deep learning.

I. INTRODUCTION

Indoor positioning and localization have emerged as a potential area for research and development during the last few years. The wide proliferation of smartphones initiated the emergence of LBS (Location-Based Services) that require precise location information of the user both outdoor and indoor. The outdoor location can be served by GPS (Global Positioning System) with high accuracy [1], however, its performance in the indoor environment is limited by many factors like signal blocking due to roofs, walls, tall buildings, and the availability of a low number of satellites in tunnels and canyons. A large number of indoor positioning technologies have been introduced that include Bluetooth [2], RFID (Radio Frequency Identification) [3], PDR (Pedestrian Dead Reckoning) [4], and Wi-Fi [5]. These technologies can be divided into two categories concerning the base infrastructure: infrastructure-dependent systems and infrastructure-independent or infrastructure-free systems. Infrastructure-dependence in this study refers to the installation of additional sensors or hardware without which these systems cannot perform fully. These technologies, however, are expensive as they require the installation of additional hardware in the environment where localization is to be performed. On the other hand, infrastructure-independent systems utilize already available resources in the form of sensors or widely available Wi-Fi APs (Access Points) to carry out the localization process. For example, the PDR

The associate editor coordinating the review of this manuscript and approving it for publication was Haiyong Zheng.

system can utilize the accelerometer and gyroscope of the smartphone to track the path of a user, still, it can provide a relative position only and always need a starting position. Recently, large-scale buildings have been designed which have a complicated structure. The performance of Wi-Fi positioning systems is affected in these complex environments due to inherent limitations of radio propagation like shadowing, and multipath, etc. and human mobility further deteriorates the performance of Wi-Fi systems [6], [7].

The geomagnetic field (referred to as the magnetic field in the rest of the paper) has emerged as a potential candidate for indoor positioning and localization. A large number of indoor localization approaches [8]–[10] have already been presented that take advantage of magnetic field data to locate a person in the indoor. These approaches work on the fingerprinting technique wherein the magnetic field magnitude is stored as fingerprints. The fingerprints are collected using the embedded magnetic sensor of the smartphone. The magnetic field is a non-radio wave resource, so it can solve the problem of radio wave interference and other similar limitations found in Wi-Fi-based localization. Additionally, it uses the natural phenomenon and resources unique to the earth, so, no additional infrastructure is required. However, the performance of magnetic field based localization systems is restricted by many factors. Existing geomagnetic field-based indoor positioning technology determines the position of the user by comparing the intensity of the geomagnetic field collected by the user with the database. However, the embedded magnetometer of the smartphone is sensitive and the collected magnetic field intensity may be very different for different smartphones. This is so because different smartphones have a different company's built-in magnetometer which results in different magnetic intensity, even for the same position. Moreover, various heights of the user result in a different magnetic intensity as well which decreases the positioning accuracy.

This study proposes the use of MP (Magnetic Pattern) and CNN (Convolutional Neural Network) to resolve the pointed out issues. The CNN is trained on MP formed at particular locations and predictions are made using the magnetic data collected by the user during the positioning phase. The contribution of this study can be summarized as follows:

- An indoor localization method is proposed which makes the use of magnetic patterns to locate a person in the indoor environment.
- CNN models are formulated to predict user indoor location. The training carried out on the magnetic patterns formed by the magnetic field intensity.
- An algorithm is devised which incorporates the predictions made from the CNNs to estimate a person's current location in the indoor.
- Extensive experiments are carried out which involve four users (two males and two females) to analyze the impact of user heights on localization performance. The training data is collected from Galaxy S8. The device dependence is evaluated using the magnetic data from Galaxy S8 and LG G6.

The composition of this paper is as follows. Section II describes the research works related to the current study. Section III gives a brief overview of geomagnetic field characteristics and its challenges while Section IV discuses the details of the proposed indoor localization approach. Section IV-D shows the details of the experimental setup used for the evaluation of the proposed method. Results are discussed in Section 3 while the conclusion is drawn in Section VI.

II. RELATED WORK

With the wide expansion of modern smartphones with embedded sensors, many indoor localization solutions have emerged, such as those utilizing activity recognition and user navigation [11]. Similarly, magnetic field-based indoor positioning systems rely on the use of a smartphone built-in magnetic sensor [12]. For example authors in [8] employ the smartphone's built-in magnetometer to collect magnetic signatures inside a building to develop the database. Later, the user collected magnetic signature is utilized to locate the user in the indoor. The proposed approach can obtain an accuracy of 2 to 6 m with a walk of 5 to 35 s. Research works [13]–[15] utilize the fingerprinting approach for indoor localization wherein the magnetic field data have been employed to make the fingerprint database. Authors in [16] investigate the methods to make distinguishable magnetic fingerprints for magnetic field-based positioning systems. A feature distinguishability measurement technique is proposed which evaluates the performance of different feature extraction methods for magnetic fingerprints.

These geomagnetic field-based indoor positioning systems use the KNN (K-Nearest Neighbor) algorithm to estimate the user's position. Indoor positioning using KNN gets K number of position candidates through matching the user magnetic signature against the magnetic database and uses K position candidates to predict the user's current location [17]. Although these techniques require a small amount of calculation and can measure the position of a user fast, yet, they suffer from lower accuracy. The accuracy decreases when the techniques are applied on heterogeneous devices, as the intensity of the geomagnetic field changes even at the same points in the positioning space. Such limitations have been investigated and several improvements have been suggested in this regard. Sensor fusion is a potential solution where the data from an accelerometer and gyroscope can be utilized to improve the localization accuracy.

Authors in [18] propose an approach that takes the benefit of a smartphone accelerometer and gyroscope to find user heading and distance information. This information is then joined with the magnetic data to increase the positioning accuracy. The approach is evaluated with heterogeneous devices and the reported positioning accuracy is 4 m at 75%. Authors in [10] leverage the use of smartphone sensors, as well as, the use of Wi-Fi APs to locate a user

in the indoor. The Wi-Fi APs are used to narrow down the search space in the magnetic database which helps to lower the localization error and elevate positioning performance. Research work [19] proposes the use of an accelerometer and gyroscope with the magnetic sensor to find the location of an indoor user. First, step detection is performed using accelerometer data. Later, the heading direction from the gyroscope and step length is fed to a magnetic field based location estimation algorithm which determines the user location. The performance is evaluated using different smartphones. Research work [20] proposes a hybrid measurement model that combines a new magnetic fingerprinting model and the existing magnitude fingerprinting. It improves system performance and does not require the calibration of different smartphone magnetometers. A refined motion model is presented as well for dynamic step length estimation to enhance the accuracy of positioning. To overcome large errors in motion estimation and improve the robustness of particle filter, the particle filter is augmented with a dynamic step length estimation algorithm and a heuristic particle resampling algorithm. The performance and results of the proposed model are promising.

Recently, the use of deep learning techniques has been reported for magnetic field-based indoor localization. Authors in [21] present an indoor localization approach that is based on the magnetic field data. It utilizes the smartphone sensors to develop the database containing fingerprints of Wi-Fi and magnetic data. Images are captured as well at each step, during the fingerprint collection. These images are then used to recognize a specific scene with the help of a Caffe trained CNN model. The recognized scenes serve as the initial estimated location which helps Wi-Fi and magnetic modules to estimate a refined position. A particle filter is later implemented to refine the location from Wi-Fi and magnetic fingerprints. Similarly, a CNN based multi-floor indoor localization approach is presented in [22] which works on multi-sensor fusion. The magnetic database is built using magnetic patterns to achieve device independence. The magnetic database search space is restricted with the CNN model which is used for floor, as well as, particular place recognition. A modified KNN approach helps to refine the localization accuracy by removing distant neighbors.

The discussed research works are limited by one or many of the following factors. The hybrid systems that use Wi-Fi to either estimate the initial location or refine the location, increase latency and are thus less appropriate for real-time localization. Moreover, with the Android 9 (Pie), the restriction on Wi-Fi scans (four scans per 2 min for foreground applications) limits the localization capability of Wi-Fi systems. Factors including obstacles, furniture, and human mobility affect the localization process of such a system as well [23], [24]. Wi-Fi positioning systems are sensitive to random noise, path loss, multipath interference and shadowing as well [25]. Moreover, iOS restriction on the Wi-Fi data from smartphones makes Wi-Fi positioning systems less attractive at the moment. Many of the above-mentioned works require a longer amount of data to calculate user position. Additionally, heterogeneous smartphones make it very complicated to design a method that can work seamlessly with different devices and provide similar positioning accuracy.

We, therefore, seek to minimize such limitations with the help of magnetic data and do not depend on Wi-Fi APs to perform localization. The magnetic data patterns are used to train CNN classifier which can predict the user location.

III. EARTH'S MAGNETIC FIELD

This section gives an overview of the magnetic field and its components, as well as, discusses the challenges in using the magnetic field data for indoor localization.

A. OVERVIEW OF THE MAGNETIC FIELD

The omnipresent phenomenon of the magnetic field on earth's surface is called the geomagnetic field and the global magnetic field intensity is distributed between 20 μT to 65 μT. The magnetic field intensity remains similar within a short space, in particular, in the outdoor. However, the presence of ferromagnetic materials like iron, steel, and steel-reinforced concrete, etc. in the indoor makes the magnetic field intensity diverse and disparate. The impact of these structures becomes more dominant as the distance to such structures decreases. These disturbances are called magnetic anomalies and have been investigated to be used as unique *signature* [26]. The magnetic field components are shown in Figure 1a while Figure 1b shows the three axes of the magnetometer sensor built into the smartphones.

The magnetic field possesses direction and magnitude and requires three parameters to represent the magnetic field at a particular point. The x, y, and z represent the north, east and downward components, respectively. An alternate representation is through the total intensity F, the inclination I, and the declination D [27], which are calculated as follows, respectively:

$$Mag_F = \sqrt{Mag_x^2 + Mag_y^2 + Mag_z^2} \tag{1}$$

$$I = \arctan(\frac{z}{H}), \quad H = \sqrt{x^2 + y^2} \tag{2}$$

$$D = \arctan(\frac{y}{x}) \tag{3}$$

B. CHALLENGES IN MAGNETIC DATA-BASED LOCALIZATION

A brief overview of the challenges in the magnetic field-based indoor localization is desirable and an analysis of the magnetic data from Galaxy S8 and LG G6 is performed in this section. These smartphones have embedded magnetic sensor and the description of each is given in Table 1. In this paper, we collect the magnetic field data at 10Hz sampling rate (new magnetic field sample every 100ms) using Google device driver API.

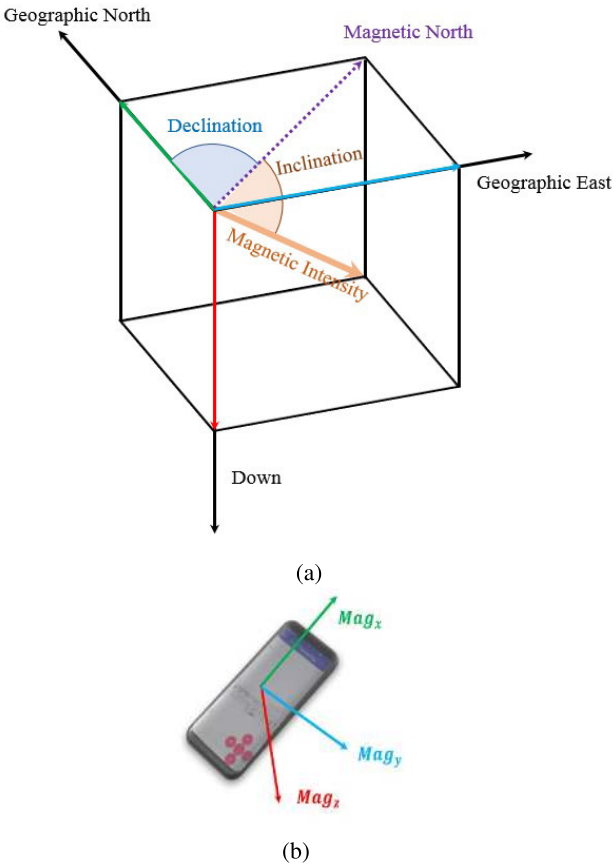

FIGURE 1. Details for magnetic field. (a) The components of earth's magnetic field, (b) axes of smartphone embedded magnetic sensor.

1) IMPACT OF TIME ON MAGNETIC FIELD

Previous research [8], [10] as well as, our experiment revealed that the magnetic field is more stable in time than that of Wi-Fi. However, the magnetic field is slightly mutated over time and hence the world magnetic model is modified every five years to accommodate the changes.

2) HOW VARIOUS SMARTPHONES BEHAVE?

The smartphones are equipped with a built-in magnetic sensor than can measure the magnetic field values at any given point, although, the values may not be the same when collected over different times. It is, however, not the impact of time, rather, the embedded magnetic sensor shows dis-similar behavior and so, the magnetic values may change during data collection and localization process. The data displayed in Fig. 2 confirms the same. However, the magnetic sensor alone is not responsible for such changes in the data, besides, shaking smartphones while walking can cause such deviations as well. The diverse behavior of the magnetic sensor and user hands' slight movements lead to different magnetic values, as can be seen as a circled area in Fig. 2. Such variations may seem slight but can potentially reduce the localization accuracy.

The magnetic field is stable over time, yet, very sensitive to the measurement device and process. Although, the

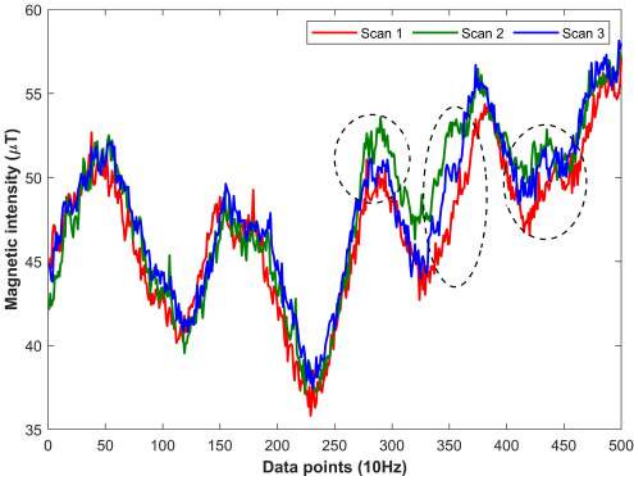

FIGURE 2. Magnetic field strength Mag_F collected during different time with Samsung Galaxy S8.

TABLE 1. Details of the magnetometer sensors used for the experiment.

Smartphone	Magnetometer	Description
Galaxy S8	AK09916C	3-axis, 16-bit, sensitivity 0.15μ T/LSB, 1.1 mA 100 Hz
LG G6	AK8963C	3-axis, 14-bit, sensitivity 0.6μ T/LSB, 2.4 mA 100 Hz

measurement mechanism is the same for all devices, even so, the embedded magnetic sensors in various smartphones are various companies manufactured and possess different sensitivity and error tolerance which makes them prone to display the different magnetic field data, even for the same location. Fig. 3 shows the magnetic data collected using Galaxy S8, and LG G6 during the same time by a person following the same trajectory, yet, the magnetic values are very different. As shown in Table 1 that the sensitivity and error tolerance for two embedded sensors are different, so, it results in different magnetic field values. Such variations in the magnetic data establish that devising a single magnetic database that can work with various smartphones seamlessly, is not appropriate as it may show various localization results even when the same localization algorithm is used.

3) IMPACT OF INDOOR STRUCTURE AND AREA

Localization accuracy of fingerprint database systems relies heavily on the uniqueness of the collected 'fingerprint' and large spaces make unique magnetic fingerprints more difficult. This is the case, especially, where the indoor structure is uniform and symmetric. The larger the area is, the higher the probability that a magnetic value may repeat itself in various locations. This phenomenon is shown in Fig. 4 where the magnetic values are shown for various locations. The circles on the graph show the locations, where the magnetic value is the same.

4) USER HEIGHT AND THE MAGNETIC DATA

Besides various smartphones, user height also has a substantial impact on the magnetic field data. Fig. 5 shows

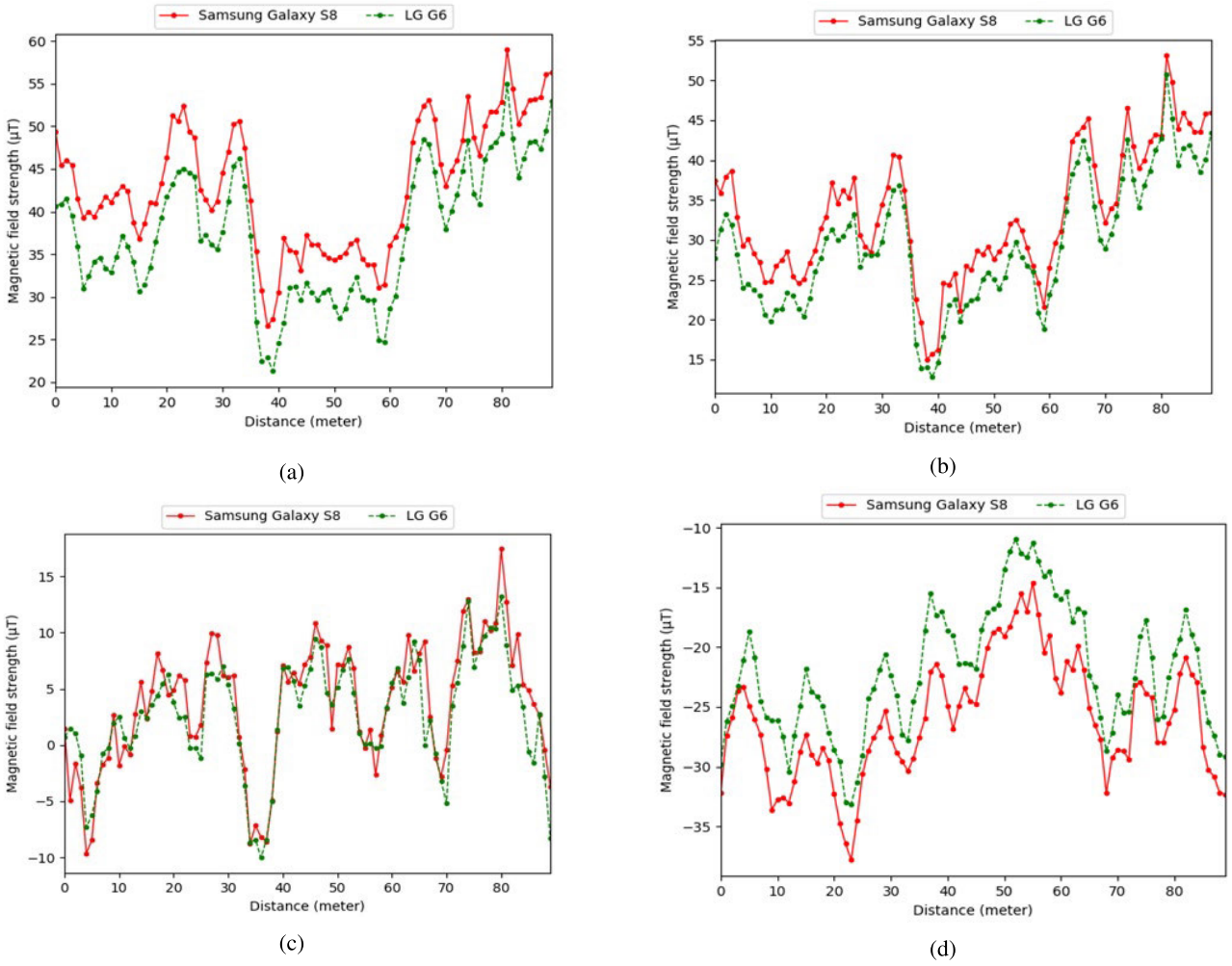

FIGURE 3. Magnetic field strength using Galaxy S8 and G6. (a) Magnetic *F*, (b) Magnetic *x*, (c) Magnetic *y*, (d) Magnetic *z*,.

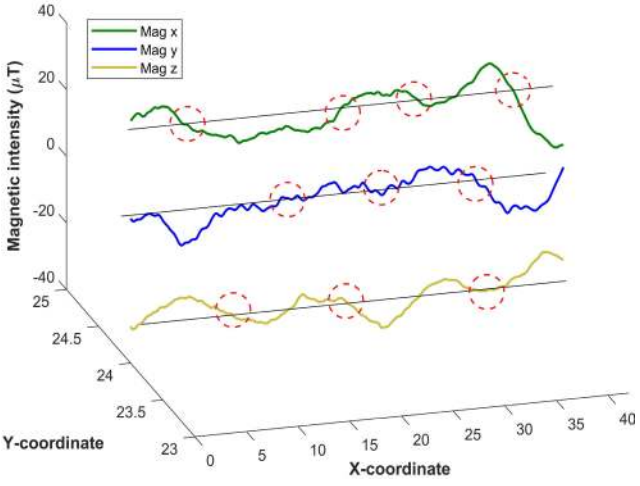

FIGURE 4. Magnetic field data showing same values for various locations.

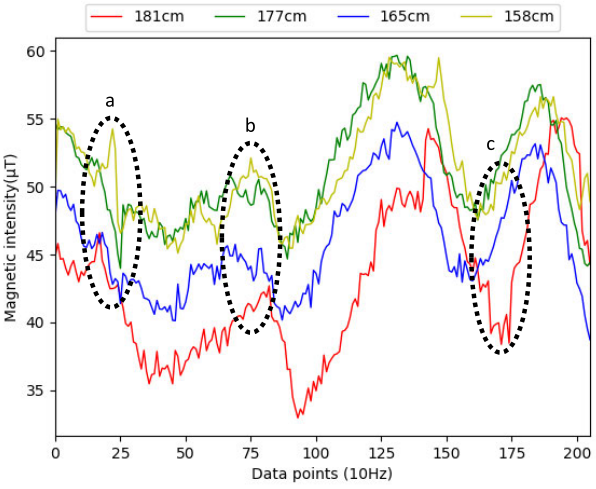

FIGURE 5. Magnetic field data collected by users of different height.

the mag_F collected from users with different heights. It displays two different phenomenons: consistent change in magnetic data and sudden change in the magnetic data. The former is on account of the user height, while the latter may occur due to either user hand movement or sensor flawed behavior.

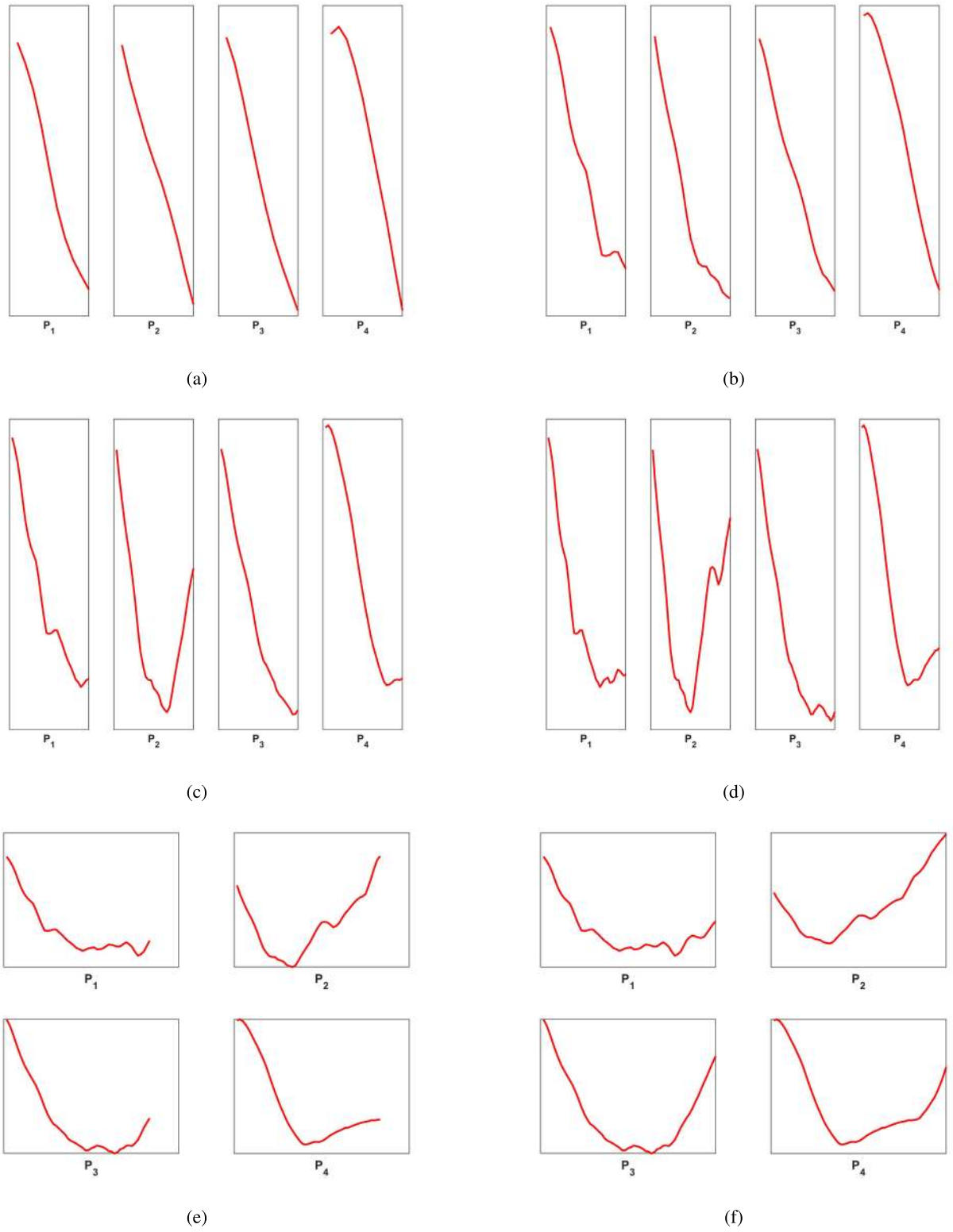

FIGURE 6. Magnetic field data using Galaxy S8. It shows only magnetic *F*, (a) Magnetic pattern with 1 m, (b) Magnetic pattern with 2 m, (c) Magnetic pattern with 3 m, (d) Magnetic pattern with 4 m, (e) Magnetic pattern with 5 m, and (f) Magnetic pattern with 6 m.

The discussed limitations of the magnetic field data make it very challenging to formulate a system using the magnetic field data, especially with a magnetic fingerprint database.

IV. PROPOSED METHOD

This section describes the details of the proposed method and the working process. We consider the magnetic field

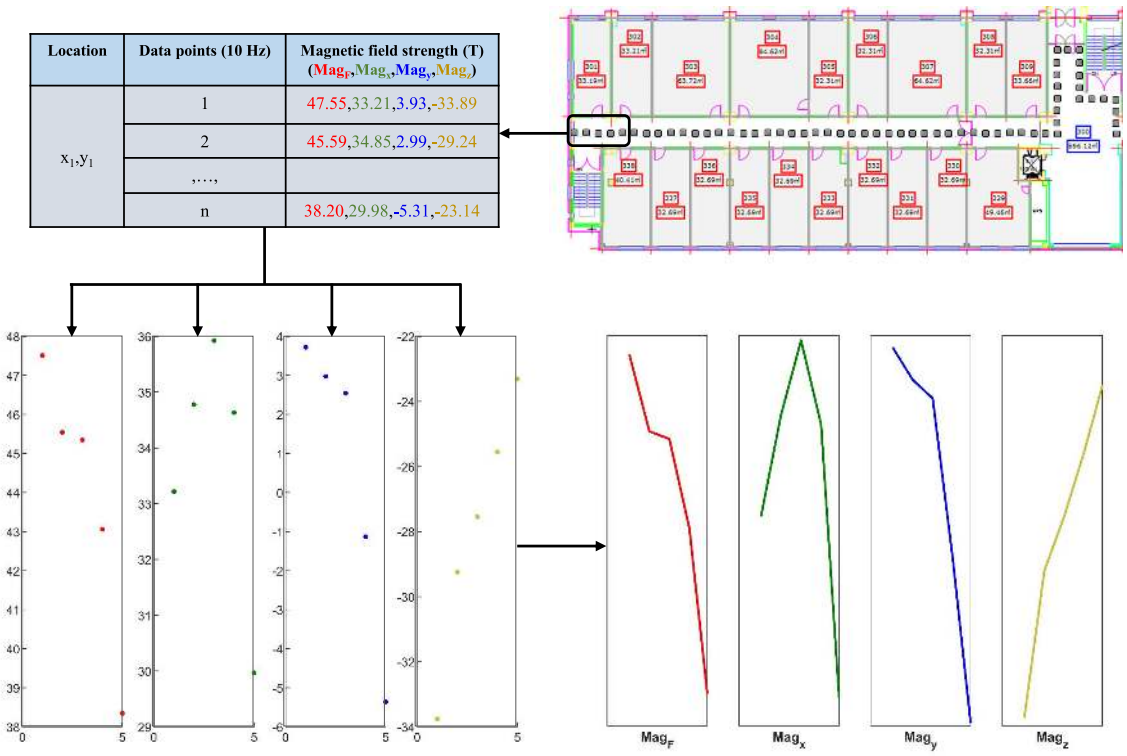

FIGURE 7. Magnetic field data collected by users of different height.

localization problem from the image processing perspective and benefit from the CNN for that purpose. The localization is followed in training and testing phases which are described separately here.

A. TRAINING PHASE

The training phase comprises of data collection, pattern making, and training using the CNN.

1) DATA COLLECTION

The data collection involves determining the ground truths and collecting the data at an appropriate sampling rate. For this purpose, we have divided the indoor area into a grid of 1 m and data is collected at 10 Hz. An accurate data collection for training can potentially improve the localization accuracy, so, instead of collecting data while walking, we collect the data at ground truth points and later perform spline interpolation to generate the intermediate values. This ensures accurate training data as against the continuous data collection which may result in different lengths and magnitude of data when collected from users of various heights.

One important aspect of training data is to determine the *fingerprint* which means that we need to determine the size of the data to be used as a feature set for a particular location. The most important quality of a fingerprint is its distinguishability or uniqueness. Increasing the size of the data to represent a location will increase the uniqueness, but it will increase the training as well as the localization time.

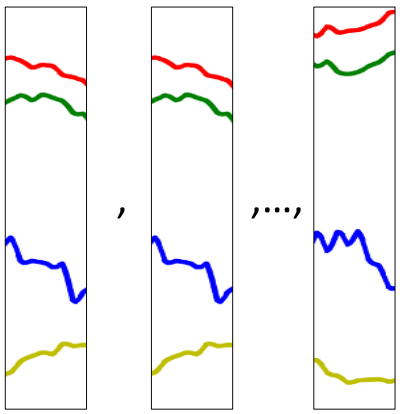

FIGURE 8. Samples of magnetic field patterns with Samsung Galaxy S8.

on the other hand, smaller data size reduces the time but affects the fingerprint uniqueness and ultimately degrades the localization accuracy. Hence, a proper fingerprint size is very critical. We analyzed various lengths of the data to determine the distinguishability and found that the magnetic data pattern is distinguishable with a 5 m pattern.

Fig. 6 shows that 1 m magnetic patterns are almost similar and make the distinction very difficult. However, as the length of the patterns is increased they become discernible. It is clear that P_1 and P_2 become dissimilar even with a length of 2 m but P_3 and P_4 look almost identical when pattern length is 3 m. With 4 m length, they become more perceptible in

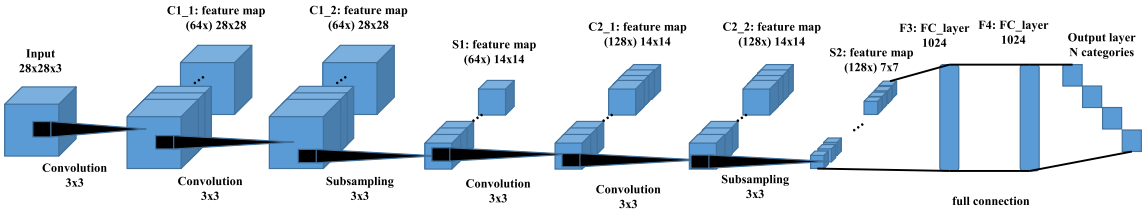

FIGURE 9. Magnetic field data collected by users of different height.

shape while 5 m patterns are distinguishable. For this reason, we used 5 m magnetic patterns to train the CNN used in this study.

2) PATTERN MAKING PROCESS

Pattern making process aims at building the magnetic patterns from the interpolated magnetic magnitude and storing it as images that are later used for training and validation. Fig. 7 shows the pattern making process. For a particular location, ground truth values for magnetic F, x, y, and z are taken and spline interpolation is performed to generate the intermediate values.

The displayed patterns shown as red, green, blue and yellow are then annotated with the location and used as the training data. Fig. 8 shows a few samples which are used for training. The patterns are stored from top to bottom starting with magnetic F and followed by x, y, and z in the given order.

3) TRAINING USING THE CNN

In this paper, the training on the magnetic field pattern (MP) is carried out using the CNN. CNN is a type of deep neural network which has shown excellent performance in recognition tasks such as computer vision [28], [29]. CNN consists of multiple layers of convolutional, pooling, and fully-connected layers, and includes activation functions, batch normalization layers, and dropout layers. Fig. 9 shows the architecture of the modeled CNN which is used in this study.

In conventional CNN, since the classification is performed using a fully connected layer as the last layer, a large amount of computation is required and the correlation between spatially adjacent data disappears. Therefore, the last layer of the proposed method classifies the input data using global average pooling (GAP), which maintains the correlation of the spatial data extracted from the previous layer. The magnetic field pattern MP is $640 \times 96 \times 3$ in size and all convolutional layers are composed of a convolutional layer, an activation function ReLU (Rectified Linear Unit), and a batch normalization layer. In the end, a Softmax layer outputs the predicted position (Pos N). Batch normalization is performed using Algorithm 1 that was proposed in [30].

The dataset is divided into training, validation and testing subsets for two buildings where the experiments are conducted. Training data is collected with Galaxy S8 while testing is performed with Galaxy S8 and LG G6. The division of the dataset and details about the number of samples are given in Table 2.

Algorithm 1 Batch Normalization [30]

Input: Values of x over a mini-batch: $\mathcal{B} = \{x_{1,\ldots,m}\}$; Parameters to be learned: γ, β

Output: $\{y_i = BN_{\gamma,\beta}(x-i)\}$

$\mu_{\mathcal{B}} \longleftarrow \frac{1}{m}\sum_{i=1}^{x} x_i$ //mini-batch mean

$\sigma^2_{\mathcal{B}} \longleftarrow \frac{1}{m}\sum_{i=1}^{x}(x_i - \mu_{\mathcal{B}})^2$ //mini-batch variance

$\widehat{x_i} \longleftarrow \frac{x_i - \mu_{\mathcal{B}}}{\sqrt{\sigma^2_{\mathcal{B}} + \epsilon}}$ //normalize

$y_i \longleftarrow \gamma\widehat{x_i} \equiv BN_{\gamma,\beta}(x_i)$ //scale and shift

TABLE 2. Details of dataset used for experiments.

Dataset	Test site	Smartphone	No. of sample
Training dataset	IT building	Galaxy S8	78,718 (8,746)
(Validation dataset)	RIC building		62,022 (6,891)
Test dataset	IT building	Galaxy S8	5,046
		LG G6	5,033
	RIC building	Galaxy S8	4,407
		LG G6	4,403

B. TESTING PHASE

The testing phase carries out data collection and normalization, and location prediction which is discussed here.

1) DATA COLLECTION AND NORMALIZATION

Test data is collected considering various perspectives including device diversity, user diversity, and time diversity, etc. The data collection conditions of the geomagnetic field for indoor positioning are set as follows:

- Use Samsung Galaxy S8 for training data and Galaxy S8 and LG G6 for testing.
- Four different users (181cm, 177cm, 165cm, 158cm), two males and two females, respectively. The users are called 'User 1', 'User 2', 'User 3', and 'User 4' to show the results.
- The height of the smartphone is fixed near the user's belt level, the direction is the direction to which the pedestrian walks arbitrarily, and the trajectory is fixed as shown in Fig. 10
- Collecting magnetic field data with large temperature differences (summer, winter), and time zones (morning, afternoon, evening).

The data collected for testing contain noise caused by the user hand's slight shaking/movements as well as, sensor's sensitivity level which needs normalization/cleaning as it may adversely affect the localization prediction. In this paper, we use the wavelet denoising technique to remove noisy data that reduces the positioning performance [31], [32].

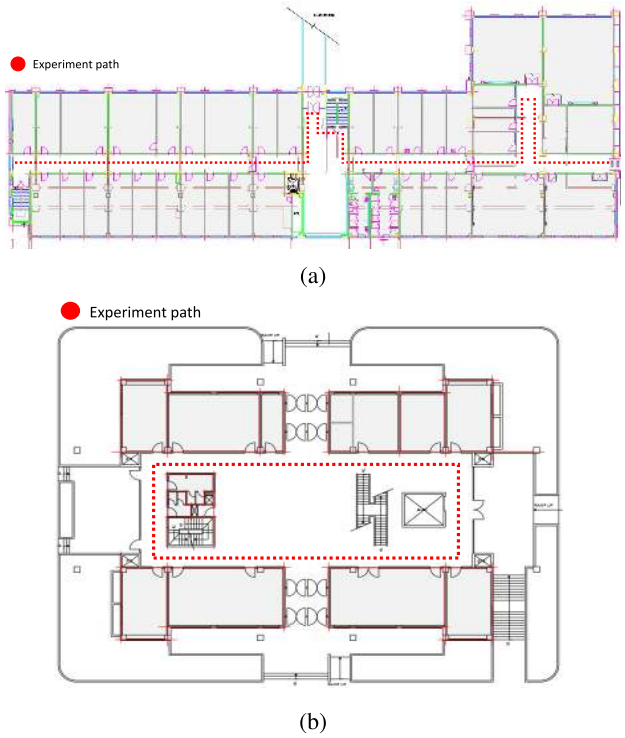

FIGURE 10. The path used for experiments. (a) IT building, (b) RIC building.

Fig. 11a shows the noisy data and Fig. 11b shows the data after applying wavelet denoising. Once the data is clean, we can transform the data into MP and feed it to the CNN model for prediction. But before we can do that we need to determine the length of the magnetic pattern, as, the MP should be from 5 m magnetic data.

The length of the MP is determined with the help of distance calculation d traveled by the user, which is achieved with two sub-procedures: step count and step length estimation. S_{l_i} shows the step length of detected step i, while S_n represents the total number of steps which are $1, 2, \ldots, n$. Step detection and heading estimation h are calculated using the algorithm proposed in [18] and is based on peak detection in the smartphone accelerometer data. After step detection, step length of *ith* step S_{l_i} is estimated with Weinberg model [33]:

$$S_{l_i} = \sqrt[k]{a_{max_i} - a_{min_i}} \tag{4}$$

where a_{max_i}, and a_{min_i} stand for the maximum and minimum acceleration, respectively and k is the step constant whose value is pre-determined during the data collection. Once step length estimation, step detection and heading estimation h is done, the distance of MP can be calculated as:

$$d = \sum_{i=1}^{n} \sqrt{(S_i \times S_{l_i} \times cos(h) + S_i \times S_{l_i} \times sin(h))^2} \tag{5}$$

Once the length of MP has been determined and it is at least five m long, then it is used as an input to the trained CNN models. The output of these models is later utilized to estimate the current position of the user in the indoor using Algorithm 2.

C. INDOOR POSITIONING TECHNIQUE USING CONVOLUTIONAL NEURAL NETWORK

This study makes use of five CNNs for user position prediction. Algorithm 2 approximates the user's current position with the help of predictions from those CNNs.

Line 1-2: Initially, m predictions from n CNNs are taken where both m and n are five. The number of m is an empirical value where the experiments revealed that top m predictions have a high probability of predicting the correct position of the user. So, P_r contains $m \times n$ values where each value represents an (x, y) position.

Line 3-8: After taking m predictions from CNNs, they need to be consolidated such that a single position can be estimated. For this purpose, a criterion similar to hard voting is defined where the frequency of each predicted position is counted. The predicted positions from one CNN are taken and compared with predictions from the rest of the CNNs to find the distance between predictions:

$$dis = \sqrt{(xi_{CNN_1} - xi_{CNN_2})^2 + (yi_{CNN_1} - yi_{CNN_2})^2} \tag{6}$$

where, dis represents the distance/error in the predictions of different CNNs. Now the frequency is increased with the following defined criteria:

$$\begin{cases} if\ dis \leq \varepsilon & \text{add frequency} \\ otherwise & \text{donot add} \end{cases} \tag{7}$$

where ε shows the error margin considered to count the frequency of a predicted position. Its value is important because a higher value would increase average positioning error but likely to reduce the maximum error and a smaller value is highly prone to higher maximum error but can substantially reduce the average error. If we set the value too high, we may be unable to have multiple occurrences of the same prediction which would ultimately affect the positioning accuracy. The value set for ε is 1 for this study and based on the empirical finding.

Algorithm 2 Position Estimation With CNN

Input: Predictions from CNNs.
Output: User's current position (x, y)

1: get m predictions P_r from n where $m, n = 1, 2, \ldots, 5$
2: get P_s for each P_r
3: **for** $i \longleftarrow$ 1 to m **do**
4: **for** $j \longleftarrow$ 1 to n **do**
5: $dis \longleftarrow calDis(P_{r_i}, P_{r_j})$
6: $P_c \longleftarrow findFreq(dis, P_{r_i}, [P_{s_i}, P_{s_j}])$
7: **end for**
8: **end for**
9: $C_p \longleftarrow makeCluster(P_c)$
10: $C_w \longleftarrow defClustWt(C_p)$
11: $P_p \longleftarrow estimatePos(C_w, C_p)$

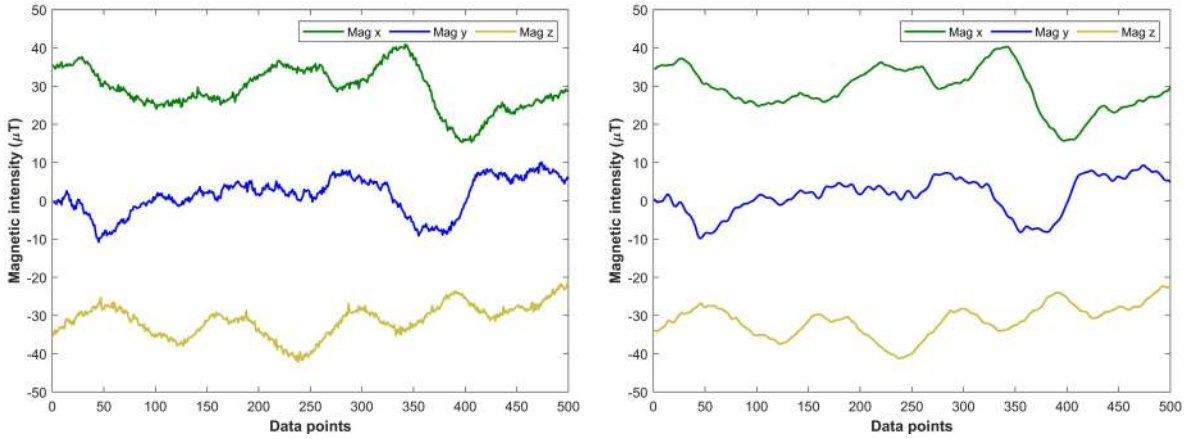

FIGURE 11. Collected magnetic field data. (a) noisy data, (b) cleaned data.

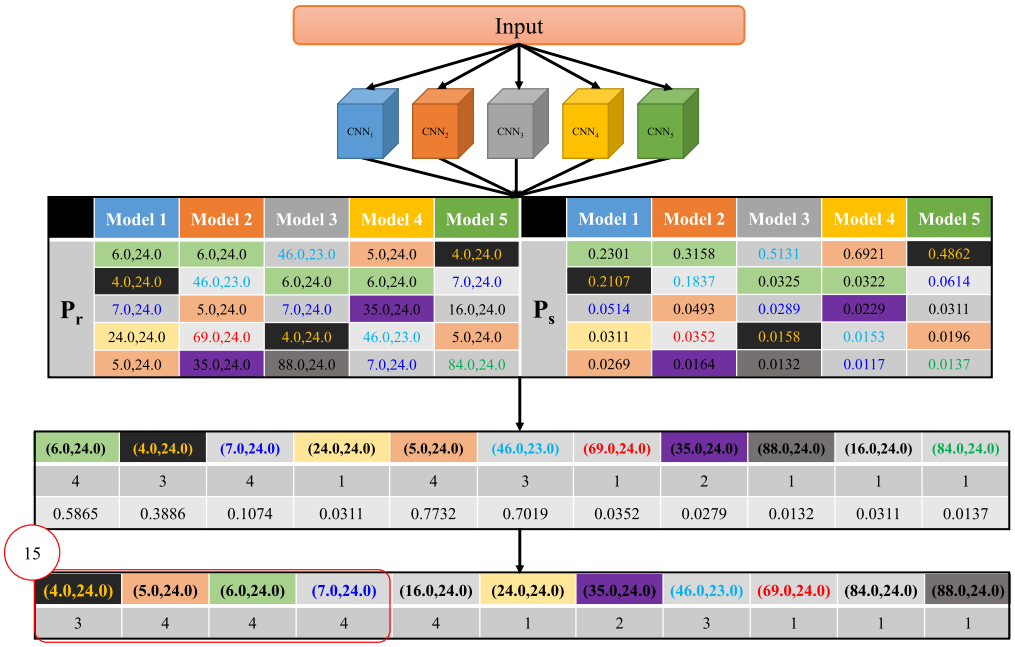

FIGURE 12. Graphical description of Algorithm 2, starting from predictions of *CNNs* to users current position estimation.

Line 9: When the count of occurrence of each prediction is completed, the predictions are clustered into C_p clusters based on their spatial closeness S_c which is the Euclidean distance between two given positions from P_c. The number of clusters depend on the sparsity of the predicted positions from CNNs. To make clusters, following criteria is used:

$$\begin{cases} if\ S_c \leq \delta & \text{add to } C_{p_i} \\ otherwise & \text{add to } \mu \end{cases} \tag{8}$$

where μ represents a set of all predictions which are sparse and do not fit in any cluster. These predictions are not considered further to estimate the user's position. The value of δ is defined empirically and set to 2, in case of larger value the cluster becomes sparse and positioning accuracy deteriorates, while the lower value may result in very small clusters which are not suitable for position estimation.

Line 10: Cluster weight is defined with two parameters: number of predictions N_{P_c} in a cluster C_{p_i} and average frequency f_a. Average frequency is calculated as follows:

$$f_a = \frac{1}{N_{P_c}} \sum_{i=1}^{N} P_c(C_{p_i}) \tag{9}$$

Line 11: The estimated position is the centroid of the cluster with higher weight. In the case of a tie, it is resolved with P_s which represents the probability score of each prediction from CNNs. At line 6 of Algorithm 2, the probability score of predicted position is added as well. The cluster with a higher average of P_s is selected for the final position.

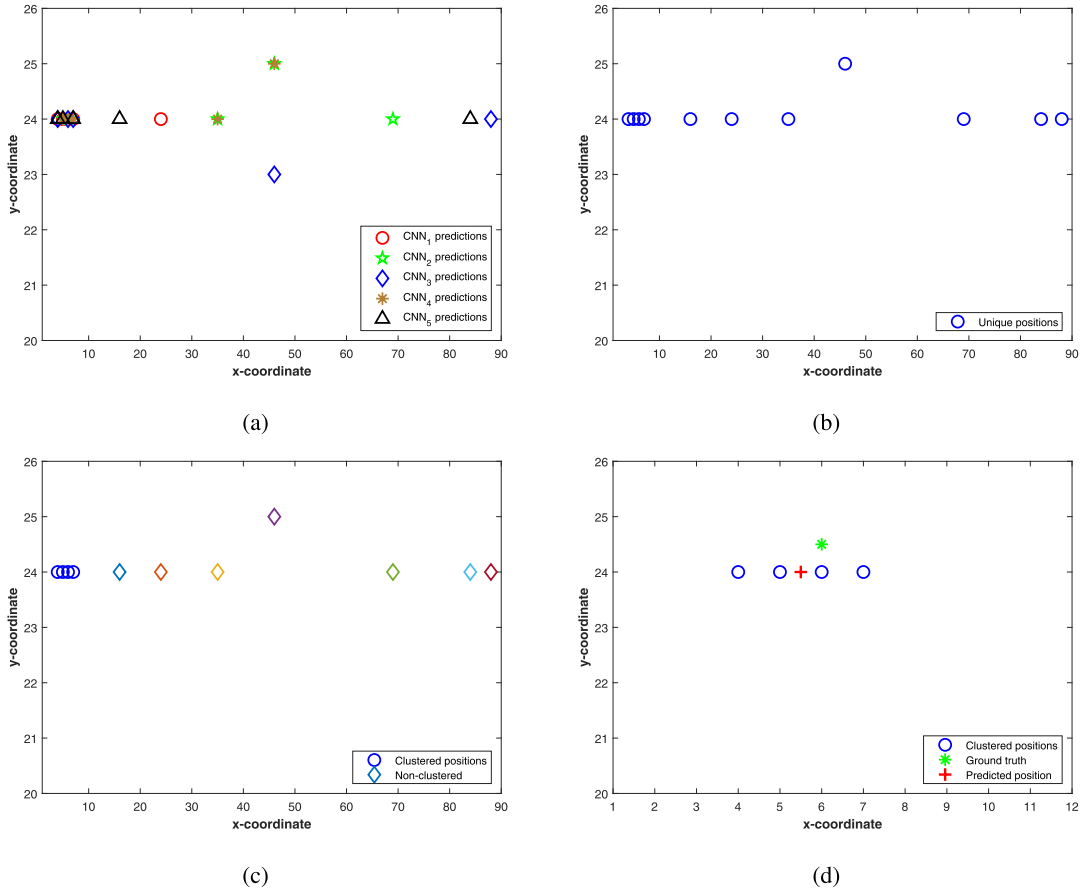

FIGURE 13. Location estimation process, (a) Top *m* predictions from all CNNs, (b) Unique predictions, (c) Clustered and unclustered positions, and (d) Cluster chosen for position estimation and final predicted position.

A working example and results are shown in Fig. 12 and Fig. 13, respectively.

D. EXPERIMENT SETUP

Experiments have been conducted in two buildings of a University campus which are separated by one kilometer. The first building is the department of Information Technology (IT) whose dimensions are 92 × 34 m and it contains a corridor in the center which is approximately 3 m wide. Testing is performed using the corridor area which is a straight path with five left turns and four right turns. The trajectory used for the IT building experiment is shown in Fig. 10a. The second building is the Industry-Academic Cooperative Technology (IACT) building and 28 m wide and 44 m long. The test corridor is 2.4 m wide and the trajectory of the experiment path is shown in Fig. 10b.

Experiments are performed with two smartphones of various brands: one from LG and is LG G6 ((LGM-G600L), and one from Samsung and is Galaxy S8 (SM-G910S). Training data is collected with Galaxy S8 alone while the testing is performed with both the smartphones. Training data is collected by 'User 1', and 'User 3', which are a male and a female, respectively and testing is performed for each user separately.

During the training data collection, the position of the smartphone is fixed, whereby the user can move in any direction but he is not allowed to change the orientation of the smartphone. The same restriction is valid for test data and this assumption has been considered by the majority of works that use the magnetic field data [10], [34], [35]. The user starting position is not known for our technique and the user may choose any arbitrary position and direction to start the walk along the defined trajectory.

V. RESULTS

A. PERFORMANCE ANALYSIS OF THE PROPOSED INDOOR POSITIONING TECHNIQUE

In this paper, various experiments are performed to evaluate the performance of the proposed technique with two perspectives: impact of different smartphones on positioning accuracy, and how different heights of various users can influence the positioning performance. So, experimental results are shown separately for various smartphones, as well as, all users who participated in the experiments. Fig. 14a and Fig. 14b shows the results for IT building with Galaxy

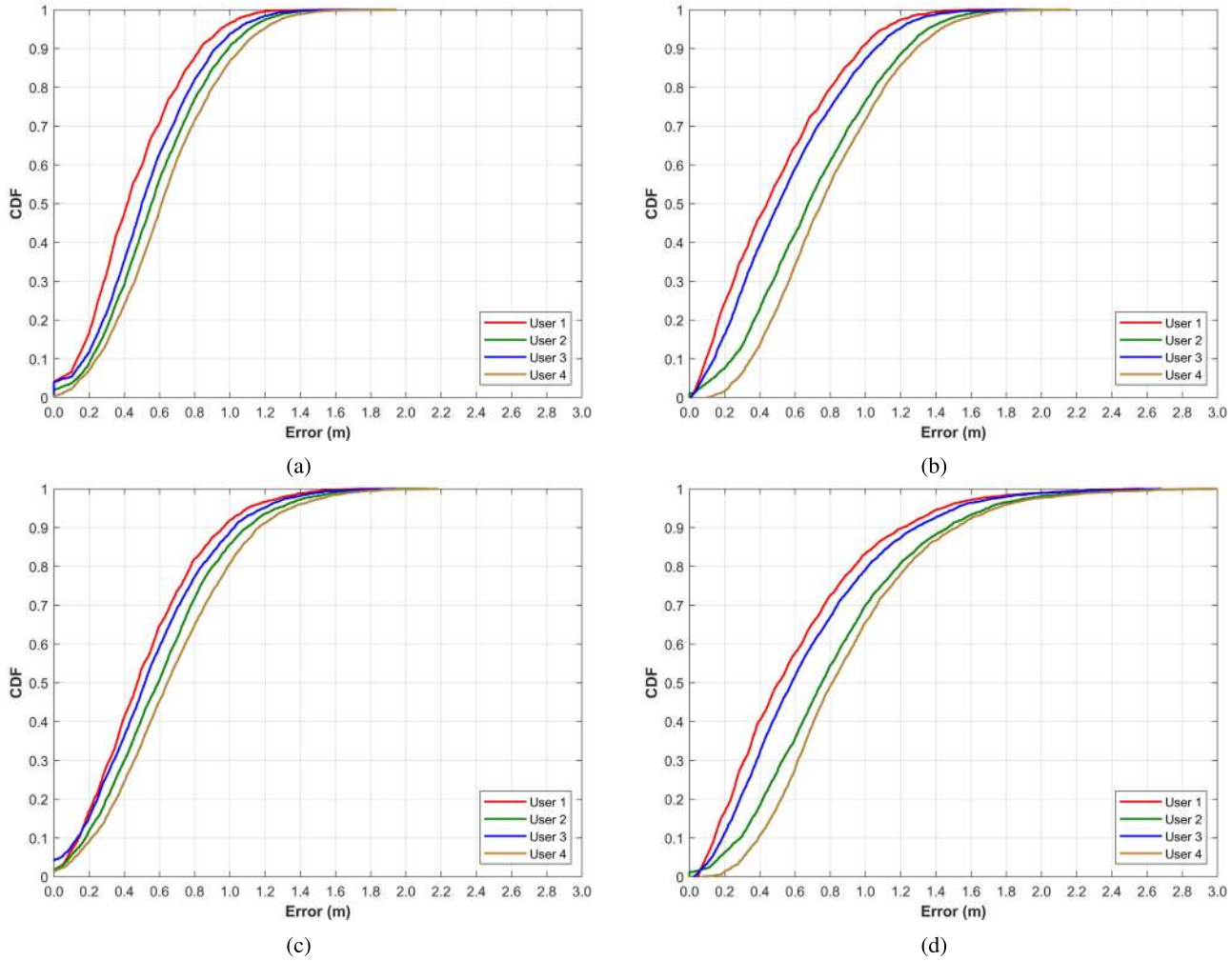

FIGURE 14. Positioning cumulative distributive function with MINLOC for individual users, (a) IT building S8, (b) IT building G6, (c) IACT building S8, and (d) IACT building G6.

S8 and LG G6, respectively, while Fig. 14c and Fig. 14d displays IACT building results, for both smartphones, respectively. There is a marginal difference in prediction accuracy when the proposed approach is tested from different users, even with the same device. Such changes may happen on account of one or more of the following reasons. First of all, we have seen in Fig. 5 that the change in magnetic patterns may occur due to change in the heights of the users which can affect the positioning accuracy of the approach slightly. Secondly, since training data contains the data collected by two users only, so in the case of data which is from those who did not take part in training can cause changes in the positioning accuracy. Thirdly, it is not guaranteed that every time we collect the data, it makes the same patterns. Magnetic patterns may vary due to the speed of the user, as well as, hands unsteady movement which can cause different positioning accuracy, every time. However, the important point is that the differences in mean and maximum errors for various users are not sky-high, rather they are almost negligible which shows the agility of the proposed approach.

TABLE 3. Details of results for IT and IACT buildings for individual users.

Test site	Smartphone	Tester	Distance error (m)		
			Mean	Max	Std. Dev.
IT building	Galaxy S8	User 1	0.45	1.71	0.27
		User 2	0.58	1.88	0.29
		User 3	0.52	1.87	0.28
		User 4	0.63	1.94	0.31
	LG G6	User 1	0.49	1.77	0.33
		User 2	0.71	1.99	0.37
		User 3	0.55	1.90	0.34
		User 4	0.79	2.16	0.35
IACT building	Galaxy S8	User 1	0.51	1.84	0.32
		User 2	0.62	2.12	0.36
		User 3	0.55	1.94	0.35
		User 4	0.67	2.18	0.37
	LG G6	User 1	0.60	2.58	0.43
		User 2	0.82	2.97	0.47
		User 3	0.67	2.68	0.44
		User 4	0.89	3.00	0.45

Fig. 14b shows the results for IT building with LG G6 and reveals that the positioning error is slightly higher than that of Galaxy S8, both in terms of mean and maximum value. We have already discussed that the user of various devices causes changes in the magnetic patterns on account of the

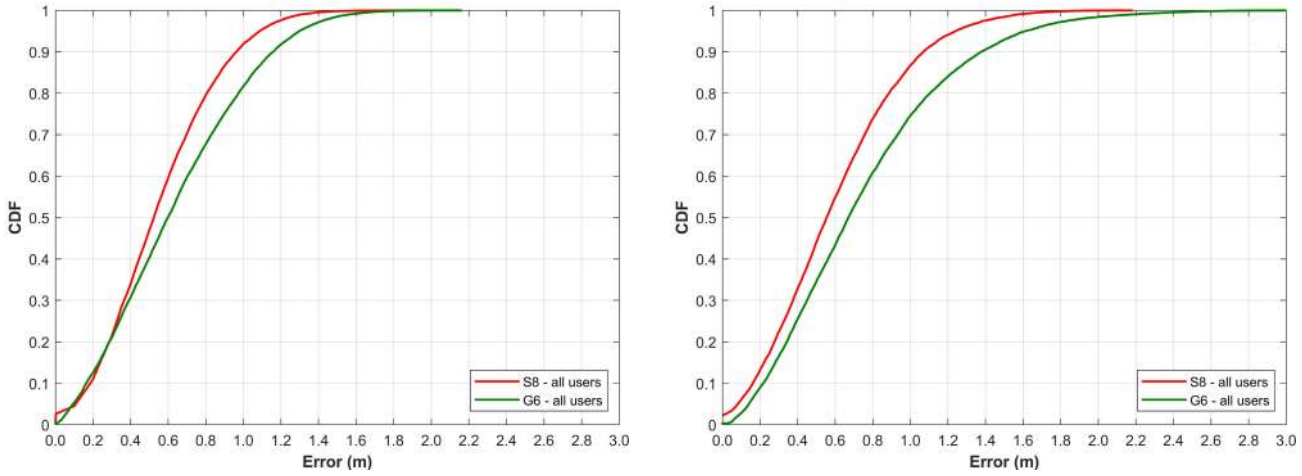

FIGURE 15. Positioning results for all users, (a) IT building, (b) IACT building.

sensitivity of the embedded magnetometer which can lead to different positioning accuracy when experiments are carried out with various smartphones. Moreover, Lg G6 data has not been included in the training process and hence the positioning error is higher. However, the proposed approach shows excellent results and the difference in positioning accuracy is marginally high for Lg G6 than that of Galaxy S8, i.e. a maximum error of 2.16 m and 1.94 m for two smartphones, respectively.

Table 3 shows the details of the results for each user separately for two buildings and two smartphones. Results show that the maxim positioning error for the IACT building is higher by a margin of 0.24 m for Galaxy S8 and 0.84 m for LG G6, respectively. The change in positioning accuracy when experimented within various buildings may occur due to a variety of factors. First, the trajectory used for the experiments may affect the positioning performance of a technique both positively and negatively. Secondly, the area of a building has an impact on the performance as well, wherein, larger areas tend to increase the positioning error. Thirdly, for the magnetic field-based localization approaches, the indoor structure of a building plays a very important role. The symmetry of the indoor environment may lead to very similar magnetic field signatures which lead to smooth and less varying magnetic patterns. As a result, the uniqueness of magnetic patterns is reduced which causes poor positioning performance. The area of the IACT building is smaller than the IT building and the most probable rationale for higher errors in IACT building is the similarity of magnetic patterns at multiple locations. Even so, the performance is very good and the maximum error in the IACT building is 2.18 m and 3.00 m for Galaxy S8 and LG G6, respectively.

Fig. 15a and Fig. 15b shows the results for all the users for IT and IACT buildings, respectively. Statistics for mean, maximum and standard deviation are shown in Table 4. The proposed approach can localize a user within 0.68 m at 50%

TABLE 4. Positioning results for IT and IACT buildings.

Test site	Smartphone	Distance error (m)				
		Mean	Max	Std. Dev.	50%	75%
IT	Galaxy S8	0.55	1.94	0.30	0.51	0.74
	LG G6	0.63	2.16	0.37	0.59	0.89
IACT	Galaxy S8	0.59	2.18	0.35	0.55	0.82
	LG G6	0.74	3.00	0.46	0.68	1.01

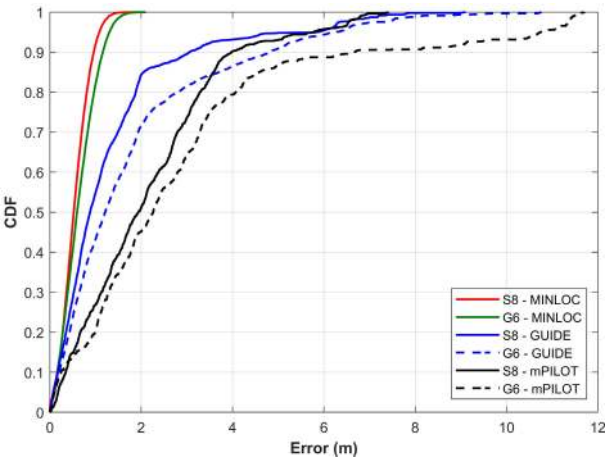

FIGURE 16. Comparison of the proposed approach with mPILOT [18], and GUIDE [19]. Results are for IT building.

with two different smartphones. The localization error at 75% is 1.01 m irrespective of the smartphone used for localization with various user heights.

B. COMPARISON OF MINLOC PERFORMANCE

The positioning performance of the proposed approach is compared with two other approaches called mPILOT [18], and GUIDE [19] which are based on the magnetic field data. These approaches utilized magnetometer, as well as, gyroscope and accelerometer data just like the proposed approach does. The results for the IT building are shown

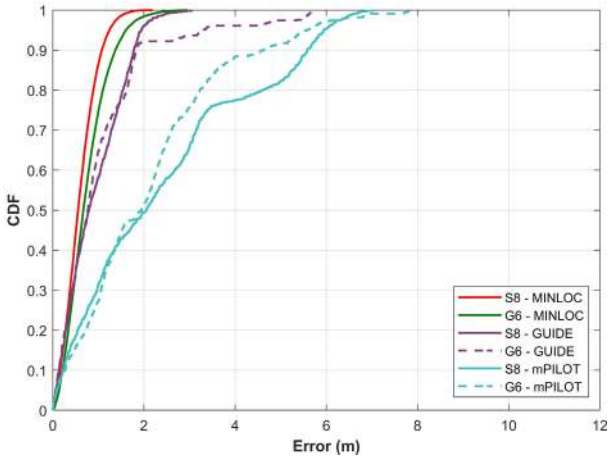

FIGURE 17. IACT building localization results comparison of the proposed approach with mPILOT [18], and GUIDE [19].

TABLE 5. Positioning results for IT and IACT buildings.

Test site	Approach	Distance error (m)			
		Mean	Max	50%	75%
IT	S8-MINLOC	0.55	1.94	0.51	0.74
	S8-GUIDE	0.89	7.87	0.87	1.77
	S8-mPILOT	1.93	7.41	1.93	3.01
	G6-MINLOC	0.63	2.16	0.59	0.89
	G6-GUIDE	0.96	8.91	0.96	1.81
	G6-mPILOT	2.96	11.69	2.26	3.40
IACT	S8-MINLOC	0.59	2.18	0.55	0.82
	S8-GUIDE	0.79	3.05	0.78	1.41
	S8-mPILOT	2.42	7.02	2.05	3.38
	G6-MINLOC	0.74	3.00	0.68	1.01
	G6-GUIDE	0.77	5.75	0.77	1.35
	G6-mPILOT	2.12	7.88	1.94	2.97

in Fig. 16. Results show that the proposed approach performs exceptionally better than both mPILOT and GUIDE. It is also noteworthy to point out the amount of data used for the proposed approach is less than half of what has been used by the compared techniques. Two important aspects to achieve the better results are the use of CNN which can perform much better when trained with large datasets than that of traditional techniques, and the voting mechanism that is presented in Algorithm 2.

Similarly, IACT building localization results shown in Fig. 17 reveal that localization results are better than mPILOT and GUIDE. Seemingly the results of GUIDE with Galaxy S8 look very similar to that of MINLOC, but mean, max, as well as 50% and 75% localization error, are much smaller for MINLOC. Detailed statistics for all approaches are shown in Table 5 which makes it clearer and easier to grasp the performance of all the approaches.

VI. CONCLUSION

This paper presents the use of CNN (Convolutional Neural Networks) to perform indoor localization with the magnetometer data from smartphones. The objectives are to mitigate the impact of various smartphones on localization accuracy and increase the performance of magnetic field based localization systems. Multiple CNNs are utilized for this purpose and their predictions are then voted with a devised technique to finally estimate the user's current position in the indoor. Contrary to traditional use of magnetic data intensity, magnetic patterns are generated and fed into CNN for training. The knowledge of the user's starting position is not required for the proposed approach. The impact of heights of various users is further investigated to analyze its impact on localization performance. Extensive experiments are performed to evaluate the performance of the proposed approach called MINLOC. Results demonstrate that MINLOC can localize a user within 1.01 m at 75%, irrespective of the smartphones (Galaxy S8, and LG G6) used and the height of the user. Results from two other approaches mPILOT and GUIDE are compared with MINLOC which shows that the proposed approach performs exceptionally well than that of other approaches. Currently, the orientation of the smartphone is fixed which can pose challenges for real-life localization, so, the localization with various orientations like call listening, phone in pocket, etc. is under study for future work. Although the proposed approach is tested with two smartphones, but we strongly believe that it has the potential to achieve identical performance for other smartphones.

VII. ACKNOWLEDGMENT

(Imran Ashraf and Mingyu Kang contributed equally to this work.)

REFERENCES

[1] N. Bulusu, J. Heidemann, and D. Estrin, "GPS-less low-cost outdoor localization for very small devices," *IEEE Pers. Commun.*, vol. 7, no. 5, pp. 28–34, Oct. 2000.
[2] V. C. Paterna, A. C. Augé, J. P. Aspas, and M. P. Bullones, "A Bluetooth low energy indoor positioning system with channel diversity, weighted trilateration and Kalman filtering," *Sensors*, vol. 17, no. 12, p. 2927, 2017.
[3] H. Xu, Y. Ding, P. Li, R. Wang, and Y. Li, "An RFID indoor positioning algorithm based on Bayesian probability and K-nearest neighbor," *Sensors*, vol. 17, no. 8, p. 1806, 2017.
[4] W. Kang and Y. Han, "SmartPDR: Smartphone-based pedestrian dead reckoning for indoor localization," *IEEE Sensors J.*, vol. 15, no. 5, pp. 2906–2916, May 2015.
[5] M. Ali, S. Hur, and Y. Park, "LOCALI: Calibration-free systematic localization approach for indoor positioning," *Sensors*, vol. 17, no. 6, p. 1213, 2017.
[6] J. Torres-Sospedra, A. Jiménez, A. Moreira, T. Lungenstrass, W.-C. Lu, S. Knauth, G. Mendoza-Silva, F. Seco, A. Pérez-Navarro, M. Nicolau, A. Costa, F. Meneses, J. Farina, J. Morales, W.-C. Lu, H.-T. Cheng, S.-S. Yang, S.-H. Fang, Y.-R. Chien, and Y. Tsao, "Off-line evaluation of mobile-centric indoor positioning systems: The experiences from the 2017 IPIN competition," *Sensors*, vol. 18, no. 2, p. 487, 2018.
[7] H. Laitinen, S. Juurakko, T. Lahti, R. Korhonen, and J. Lahteenmaki, "Experimental evaluation of location methods based on signal-strength measurements," *IEEE Trans. Veh. Technol.*, vol. 56, no. 1, pp. 287–296, Jan. 2007.
[8] K. P. Subbu, B. Gozick, and R. Dantu, "LocateMe: Magnetic-fields-based indoor localization using smartphones," *ACM Trans. Intell. Syst. Technol.*, vol. 4, no. 4, pp. 1–27, Sep. 2013.
[9] I. Ashraf, S. Hur, and Y. Park, "Mdirect-magnetic field strength and pedestrian dead reckoning based indoor localization," in *Proc. Int. Conf. Indoor Positioning Indoor Navigat. (IPIN)*, Nantes, France, 2018, pp. 24–27.
[10] Y. Shu, C. Bo, G. Shen, C. Zhao, L. Li, and F. Zhao, "Magicol: Indoor localization using pervasive magnetic field and opportunistic WiFi sensing," *IEEE J. Sel. Areas Commun.*, vol. 33, no. 7, pp. 1443–1457, Jul. 2015.
[11] B. Shin, C. Kim, J. Kim, S. Lee, C. Kee, and T. Lee, "Motion recognition based 3D pedestrian navigation system using smartphone," *IEEE Sensors J.*, vol. 16, no. 18, pp. 6977–6989, 2016.

[12] S. Hur and Y. Park, "A study on application of geo-magnetism field for improving indoor positioning accuracy," *The J. Korean Inst. Commun. Inf. Sci.*, vol. 34, no. 4, pp. 25–32, 2017.
[13] E. Le Grand and S. Thrun, "3-axis magnetic field mapping and fusion for indoor localization," in *Proc. IEEE Int. Conf. Multisensor Fusion Integr. Intell. Syst. (MFI)*, Sep. 2012, pp. 358–364.
[14] J. Haverinen and A. Kemppainen, "Global indoor self-localization based on the ambient magnetic field," *Robot. Auto. Syst.*, vol. 57, no. 10, pp. 1028–1035, Oct. 2009.
[15] J. Song, H. Jeong, S. Hur, and Y. Park, "Improved indoor position estimation algorithm based on geo-magnetism intensity," in *Proc. Int. Conf. Indoor Positioning Indoor Navigat. (IPIN)*, Oct. 2014, pp. 741–744.
[16] W. Shao, F. Zhao, C. Wang, H. Luo, T. Muhammad Zahid, Q. Wang, and D. Li, "Location fingerprint extraction for magnetic field magnitude based indoor positioning," *J. Sensors*, vol. 2016, pp. 1–16, Dec. 2016.
[17] J. Chung, M. Donahoe, C. Schmandt, I.-J. Kim, P. Razavai, and M. Wiseman, "Indoor location sensing using geo-magnetism," in *Proc. 9th Int. Conf. Mobile Syst., Appl., Services (MobiSys)*, 2011, pp. 141–154.
[18] I. Ashraf, S. Hur, and Y. Park, "MPILOT-magnetic field strength based pedestrian indoor localization," *Sensors*, vol. 18, no. 7, p. 2283, 2018.
[19] I. Ashraf, S. Hur, M. Shafiq, S. Kumari, and Y. Park, "GUIDE: Smartphone sensors-based pedestrian indoor localization with heterogeneous devices," *Int. J. Commun. Syst.*, vol. 32, no. 15, p. e4062, Oct. 2019.
[20] H. Xie, T. Gu, X. Tao, H. Ye, and J. Lv, "MaLoc: A practical magnetic fingerprinting approach to indoor localization using smartphones," in *Proc. ACM Int. Joint Conf. Pervas. Ubiquitous Comput. UbiComp Adjunct*, 2014, pp. 243–253.
[21] M. Liu, R. Chen, D. Li, Y. Chen, G. Guo, Z. Cao, and Y. Pan, "Scene recognition for indoor localization using a multi-sensor fusion approach," *Sensors*, vol. 17, no. 12, p. 2847, 2017.
[22] I. Ashraf, S. Hur, and Y. Park, "Application of deep convolutional neural networks and smartphone sensors for indoor localization," *Appl. Sci.*, vol. 9, no. 11, p. 2337, 2019.
[23] L. Sun, Z. Zheng, T. He, and F. Li, "Multifloor Wi-Fi localization system with floor identification," *Int. J. Distrib. Sensor Netw.*, vol. 11, no. 7, Jul. 2015, Art. no. 131523.
[24] M. A. Bitew, R.-S. Hsiao, H.-P. Lin, and D.-B. Lin, "Hybrid indoor human localization system for addressing the issue of RSS variation in fingerprinting," *Int. J. Distrib. Sensor Netw.*, vol. 11, no. 3, Mar. 2015, Art. no. 831423.
[25] A. Bensky, *Wireless Positioning Technologies and Applications*. Norwood, MA, USA: Artech House, 2016.
[26] B. Li, T. Gallagher, A. G. Dempster, and C. Rizos, "How feasible is the use of magnetic field alone for indoor positioning?" in *Proc. Int. Conf. Indoor Positioning Indoor Navigat. (IPIN)*, Nov. 2012, pp. 1–9.
[27] E. L. Gunnarsdóttir, "The earth's magnetic field," Ph.D. dissertation, School Eng. Natural Sci., Univ. Iceland, Reykjavik, Iceland, 2012.
[28] A. Krizhevsky, I. Sutskever, and G. E. Hinton, "Imagenet classification with deep convolutional neural networks," in *Proc. Adv. Neural Inf. Process. Syst.*, 2012, pp. 1097–1105.
[29] S. Ren, K. He, R. Girshick, and J. Sun, "Faster R-CNN: Towards real-time object detection with region proposal networks," in *Proc. Adv. Neural Inf. Process. Syst.*, 2015, pp. 91–99.
[30] S. Ioffe and C. Szegedy, "Batch normalization: Accelerating deep network training by reducing internal covariate shift," 2015, *arXiv:1502.03167*. [Online]. Available: http://arxiv.org/abs/1502.03167
[31] B. Gnedenko, "Sur la distribution limite du terme maximum D'Une serie aleatoire," *Ann. Math.*, vol. 44, no. 3, pp. 423–453, Jul. 1943.
[32] D. L. Donoho, "De-noising by soft-thresholding," *IEEE Trans. Inf. Theory*, vol. 41, no. 3, pp. 613–627, May 1995.
[33] H. Weinberg, "Using the ADXL202 in pedometer and personal navigation applications," *Analog Devices*, vol. 2, no. 2, pp. 1–6, 2002.
[34] J. Bird and D. Arden, "Indoor navigation with foot-mounted strapdown inertial navigation and magnetic sensors [emerging opportunities for localization and yracking]," *IEEE Wireless Commun.*, vol. 18, no. 2, pp. 28–35, Apr. 2011.
[35] C. Galván-Tejada, J. García-Vázquez, J. Galván-Tejada, J. Delgado-Contreras, and R. Brena, "Infrastructure-less indoor localization using the microphone, magnetometer and light sensor of a smartphone," *Sensors*, vol. 15, no. 8, pp. 20355–20372, 2015.

IMRAN ASHRAF received the Ph.D. degree in information and communication engineering from Yeungnam University, South Korea, in 2018, and the M.S. degree in computer science from the Blekinge Institute of Technology, Karlskrona, Sweden, in 2010. He has worked as a Postdoctoral Fellow at Yeungnam University, Gyeongsan, South Korea, where he is currently an Assistant Professor with the Information and Communication Engineering Department. His research interests include indoor positioning and localization, indoor location-based services in wireless communication, and data mining.

MINGYU KANG received the bachelor's and master's degrees in information and communication engineering from Yeungnam University, South Korea, in 2017 and 2019, respectively. His research interests include deep learning especially convolutional neural networks for indoor positioning and image processing.

SOOJUNG HUR received the B.S. degree from Daegu University, Gyeongbuk, South Korea, in 2001, the M.S. degree in electrical engineering from the San Diego State University of San Diego, in 2004, and the M.S. and Ph.D. degrees in information and communication engineering from Yeungnam University, South Korea, in 2007 and 2012, respectively. She is currently working as a Research Professor with the Mobile Communication Laboratory, Yeungnam University. Her current research interests include the performance of mobile communication, indoor/outdoor location, and unnamed vehicle.

YONGWAN PARK received the B.E. and M.E. degrees in electrical engineering from Kyungpook University, Daegu, South Korea, in 1982 and 1984, respectively, and the M.S. and Ph.D. degrees in electrical engineering from the State University of New York at Buffalo, USA, in 1989 and 1992, respectively. He was a Research Fellow with the California Institute of Technology, from 1992 to 1993. From 1994 to 1996, he was a Chief Researcher for developing the IMT-2000 system, SK Telecom, South Korea. Since 1996, he has been a Professor of information and communication engineering with Yeungnam University, South Korea. From January to February of 2000, he was an Invited Professor with the NTT DoCoMo Wireless Laboratory, Japan. He was Visiting Professor with UC Irvine, USA, in 2003. From 2008 to 2009, he was the Director of the Technology Innovation Center for Wireless Multimedia by the Korean Government. From 2009 to March 2017, he was the President of Gyeongbuk Institute of IT Convergence Industry Technology (GITC), South Korea. He is the Chairman of the 5G Forum Convergence Service Committee, South Korea. His current research interests include 5G systems in communication, OFDM, PAPR reduction, indoor location-based services in wireless communication, and smart sensors (LIDAR) for smart cars.